SAND2015-6810C

Design Optimization for Miniature Nuclear Reactors

Sal Rodriguez and David Ames

Sandia National Labs, P.O. Box 5800, MS-1136, Albuquerque, NM 87185-1136, sbrodri@sandia.gov

INTRODUCTION

Generation III/III+ light water reactors (LWRs) are complex and require significant expertise for safe operation. Despite myriads of safety margins, regulations, and precautions, three severe accidents have resulted in billions of dollars' worth of losses, contamination, and have contributed to the decision by Germany and Switzerland to discontinue nuclear power. New small modular reactors (SMRs) and Generation IV reactors reduce complexity and add inherent safety measures. However, in terms of total cost (including safety), these reactors would result in higher costs if severe accidents occurred. Furthermore, their power output may not be economically competitive with other energy sources.[1] Recent advances in nuclear engineering and materials strongly suggest that many of these economics and safety issues can be significantly mitigated, if not eliminated, with miniature nuclear reactors (MNRs). MNR size could range from the smallest achievable critical mass to about 10 times smaller than an SMR (a few kW to several 10s MW).

There has been a significant increase recently in the research of small reactors.[2-5] According to Hyperion Power[2], their MNR can be built for ~$50 million (vs. 6 to $10 billion for LWRs). *Therefore, MNRs could be scaled so they are the right size and cost for a given application.* Thus, MNRs have the potential for being relatively-inexpensive reactors for small grids, isotope production, test reactors for materials testing, co-generation heating, desalination, and hydrogen production; see Fig. 1.

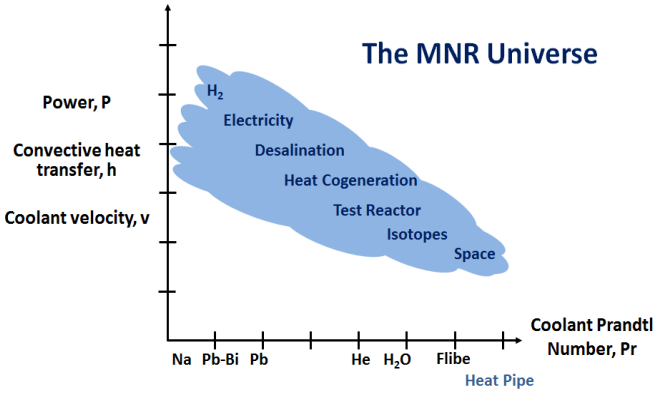

Fig. 1. The diverse opportunities afforded by MNRs.

Because reactor designs are complex and costly to perform detailed analysis, it is important to be able to estimate their behavior with simplified analytical equations. Once a promising design is found, the analysis can be refined with multi-physics computation and field experiments. For this research, we investigated various momentum, energy, and neutronics equations that can be used readily to perform preliminary MNR design calculations. Towards this goal, Eqns. 11, 13A, 13B, 15A, 15B, and 18 were developed assuming that the MNR is under laminar, natural circulation. Later, more complex 3D multi-physics calculations can be used to refine a pre-qualified MNR design, using computational fluid, thermal, and structural dynamics, as well as safety, neutronics, and economic analysis, all of which are at our disposal.

DESCRIPTION OF THE ACTUAL WORK

For this research, we begin by investigating the potential of various metal coolants, with the goal of seeking the most appropriate coolants based on their ability to provide sufficient flow and heat transfer under natural circulation in the primary system. We also investigated various key fuels and related parameters, including uranium nitride and uranium dioxide, fuel enrichment, and neutron velocity.

Because our MNR design will rely solely on natural circulation in the primary system near atmospheric pressure, forced-circulation coolant pumps and associated equipment will not be required, thereby reducing cost; this has the added advantage of having a higher safety signature. The other advantage, of course, is that the smaller the core, the harder it will be for it to cause expensive severe accidents; by contrast, it is expected that the power output will become more expensive. Indeed, this is an optimization issue.

Unless special design features are incorporated into our MNR design, natural circulation flow through the core will tend to be laminar. Therefore, methods to enhance heat transfer are desirable. We propose a solution that uses helical ribs to induce turbulence through swirl, and thereby provide enhanced heat transfer and higher power output efficiency.[6]

Momentum and Energy Conservation under Natural Circulation

Consider a Cartesian system under natural circulation subject to conservation of momentum and energy. Due to symmetry, it is reasonable to consider a 2D system, as shown in Fig. 2, with a surface at a given temperature, T_w that induces coolant flow due to buoyancy. Then, conservation of momentum under laminar, natural circulation is:

$$\rho\frac{\partial u}{\partial t}+\rho\left(u\frac{\partial u}{\partial x}+\mathrm{v}\frac{\partial u}{\partial y}\right)=\mu\frac{\partial^2 u}{\partial y^2}-\frac{\partial P}{\partial x}-\rho g_x \quad (1)$$

u=velocity in the x-direction
v=velocity in the y-direction
ρ=density
μ=dynamic viscosity
g=gravitational constant

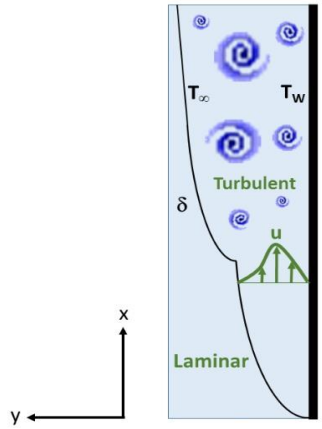

Fig. 2. Boundary layer generated by a heated wall.

The conservation of energy equation is:

$$\frac{\partial T}{\partial t}+\vec{V}\bullet\vec{\nabla}T=\frac{\dot{q}_s'''}{\rho C_p}+\alpha\nabla^2 T \quad (2A)$$

or, in 2D with no heat source,

$$\frac{\partial T}{\partial t}+u\frac{\partial T}{\partial x}+\mathrm{v}\frac{\partial T}{\partial y}=\frac{k}{\rho C_p}\frac{\partial^2 T}{\partial y^2} \quad (2B)$$

T = fluid temperature

k=fluid thermal conductivity

C_p = fluid heat capacity

$\alpha=\frac{k}{\rho C_p}$.

The Grashof (Gr) number is defined as:

$$Gr=\frac{\beta \mathrm{g} \mathrm{x}^3 \Delta \mathrm{T}}{\nu^2} \quad (3)$$

where β=fluid thermal expansion coefficient:

$$\beta\equiv-\frac{1}{\rho}\left(\frac{\partial\rho}{\partial T}\right)_P\approx-\frac{1}{\rho}\frac{(\rho-\rho_\infty)}{(T-T_\infty)}=\frac{1}{\rho}\frac{(\rho_\infty-\rho)}{(T-T_\infty)} \quad (4)$$

or

$$\rho_\infty-\rho=\rho\beta(T-T_\infty) \quad (5)$$

h=wall height

$\Delta \mathrm{T}=T_w-T_\infty$

T_w = temperature of wall that heats the fluid

$\nu=\frac{\mu}{\rho}$=fluid kinematic viscosity

T_∞ = fluid temperature far away from the wall.

The fluid motion results from the density-induced pressure gradient,

$$\frac{\partial P}{\partial x}=-\rho_\infty g_x \quad (6)$$

Substituting (5) and (6) into (1), we obtain:

$$\rho\frac{\partial u}{\partial t}+\rho\left(u\frac{\partial u}{\partial x}+\mathrm{v}\frac{\partial u}{\partial y}\right)=\mu\frac{\partial^2 u}{\partial y^2}+g_x(\rho_\infty-\rho)= \quad (7)$$

$$\mu\frac{\partial^2 u}{\partial y^2}+g_x\left[\rho\beta(T-T_\infty)\right]$$

Let a cubic polynomial solution be assumed in the form of the product of two equations, each being a function of a single coordinate (separation of variables),

$$\mathrm{u(x,y)}=U(x)\left(a+by+cy^2+dy^3\right) \quad (8)$$

Applying the appropriate boundary conditions, the solution to (7) based on polynomial (8) is[7]:

$$\mathrm{u(x,y)}=\frac{\beta\delta^2 \mathrm{g}(T_w-T_\infty)}{4\nu}\frac{y}{\delta}\left(1-\frac{y}{\delta}\right)^2 \quad (9)$$

$\delta=\delta(x)=\mathrm{Ax}^{1/4}$=thermal boundary layer thickness (10A)

Parameter A is a function of the coolant physical properties,

$$\mathrm{A}=3.93\left(\frac{20}{21}+\frac{\nu}{\alpha}\right)^{1/4}\left[\frac{g_x\beta(T_w-T_\infty)}{\nu^2}\right]^{-1/4}\left(\frac{\nu}{\alpha}\right)^{-1/2} \quad (10B)$$

Thus, the boundary layer thickness can be found via Eqns. 10A and B, while the coolant velocity at any location (x,y) is determined from Eqn. 9. However, by taking the derivative of u with respect to y in Eqn. 9 and setting it to 0, we can obtain the value of y where u is maximum:

$$\frac{\mathrm{du}}{\mathrm{dy}}=0=\left[\frac{\beta\delta^2 \mathrm{g}(T_w-T_\infty)}{4\nu}\right]\left(\frac{1}{\delta}-4\frac{y}{\delta^2}+3\frac{y^2}{\delta^3}\right)$$

$$\Rightarrow y=\frac{\delta}{3}.$$

In other words, for any location x, there is a maximum peak velocity u, which is always located at y=δ/3. Thus, the maximum velocity $\mathrm{u}_{\max}$(x) is:

$$\mathrm{u}_{\max}\left(\mathrm{x},\mathrm{y}=\frac{\delta}{3}\right)=\frac{\beta\delta^2 \mathrm{g}(T_w-T_\infty)}{4\nu}\left(\frac{4}{27}\right)=\frac{\beta\delta^2 \mathrm{g}(T_w-T_\infty)}{27\nu} \quad (11)$$

To the author's knowledge, Eqn. 11 has not been cited previously in the literature; the same goes for Eqns. 13A, 13B, 15A, 15B, and 18, which will be presented shortly. Table I compares a computational fluid dynamics calculation using Fuego vs. Eqn. 11. The computational output was compared for water with Prandtl number (Pr) in the range of 1.1 to 6.1. Note that for a vertical plate, $\mathrm{GrPr}<10^9$ implies laminar natural circulation, while $\mathrm{GrPr}>10^9$ implies turbulent natural circulation.[7] Eqn. 11 is suitable for systems with Pr~1.0, which is the case for many gases and water. However, it should not be used when Pr<<1, which is the case for molten metal coolants. This situation will be treated next.

Table I. Validation of the Fuego Natural Circulation Model (fluid=water).

T_{wall} (K)	Eqn. 11 Peak Velocity (m/s)	Fuego Peak Velocity (m/s)	Error (%)	Gr	Pr
350	0.0199	0.0223	10.8	$3.2\text{x}10^6$	6.1
400	0.0388	0.0421	7.8	$9.4\text{x}10^6$	3.4
500	0.0648	0.0695	7.3	$3.5\text{x}10^7$	1.6
600	0.14	0.138	1.4	$1.62\text{x}10^8$	1.1

The velocity distribution can also be obtained from the work of Ostrach[8], who solved the same system as Holman[7]. However, rather than providing an analytical solution, Ostrach tabulated values for dimensionless velocity f', temperature H', and position η. Based on Eqn. 11, it is clear that for any location x, there is a maximum velocity u. Following this premise, it was found in Ostrach's output that for a given Pr and η, there was a maximum f', as expected. Ostrach calculated f' for Pr=0.01, 0.72, 0.733, 1, 2, 10, 100, and 1,000, so maximum values were obtained from his tables. However, because molten metals can have values in the range of 0.001<Pr<0.01, additional values of f' were computed by the authors. Then, the peak f' for each Pr was selected, and a curve fit based on

$$\mathrm{f}'_{\max}=\mathrm{f}'(\mathrm{Pr}) \qquad (12)$$

using a power curve fit obtained from Matlab was obtained,

$$\mathrm{f}'_{\max}=0.5\,\mathrm{Pr}^{-0.11}-0.24 \qquad (13A)$$

A more complex, rational function can also be used to obtain a closer fit to the data,

$$\mathrm{f}'_{\max}=\frac{1.85\,\mathrm{Pr}+0.23}{0.65\,\mathrm{Pr}^2+6.5\,\mathrm{Pr}+0.36}+0.015 \qquad (13B)$$

From Ostrach,

$$\mathrm{f}'(\eta)\equiv\frac{\frac{ux}{\nu_\infty}}{2\sqrt{Gr_x}} \qquad (14)$$

Substituting Eq. 13 into 14 and solving for the peak velocity u_{max},

$$u_{\max}(x)=2\mathrm{f}'_{\max}(\eta)\frac{\nu_\infty}{x}\sqrt{Gr_x}$$

Thus,

$$u_{\max}(x)=2\left(0.5\,\mathrm{Pr}^{-0.11}-0.24\right)\frac{\nu_\infty}{x}\sqrt{Gr_x} \qquad (15A)$$

or

$$u_{\max}(x)=2\left(\frac{1.85\,\mathrm{Pr}+0.23}{0.65\,\mathrm{Pr}^2+6.5\,\mathrm{Pr}+0.36}+0.015\right)\frac{\nu_\infty}{x}\sqrt{Gr_x} \qquad (15B)$$

Fig. 3. shows the f' vs. Pr for Pr ranging from 0 to 5 and from 0 to 500. In this range, Eqn. 15A is typically within 10% error of the computed values, while 15B is primarily within 5% or less. As expected, Fig. 3 shows that the peak fluid velocity induced via natural circulation increases as Pr decreases. This shows that all things being equal, Na has a higher peak velocity, which has a higher peak velocity than Pb-Bi, which in turn has a higher peak velocity than Pb. However, from Ostrach, higher Pr results in higher Nusselt number (Nu), and therefore more heat transfer, as follows.

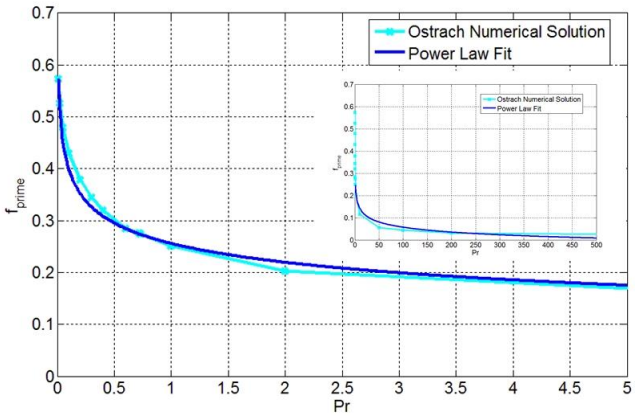

Fig. 3. Dimensionless velocity vs. Pr.

Again, from Ostrach,

$$-H'(0)\equiv\frac{Nu_x}{\left(\frac{Gr_x}{4}\right)^{1/4}} \qquad (16)$$

Similar to the development of a curve fit for momentum, we obtained the following expression for H'(0) from the Ostrach data using Matlab:

$$H'(0)=-0.6\mathrm{Pr}^{0.28} \qquad (17)$$

$$Nu_x=\frac{hx}{k}=-H'(0)\left(\frac{Gr_x}{4}\right)^{1/4}=0.6\mathrm{Pr}^{0.28}\left(\frac{Gr_x}{4}\right)^{1/4} \qquad (18)$$

Fig. 4 shows the Ostrach numerical solution for H'(0) vs. Pr. Whereas rectangular geometry was used to obtain the above results, it noted here that correction factors for Cartesian to cylindrical geometry are readily available, if a more refined analysis is desired.[7] Finally, the fuel temperature distribution can be estimated for a cylindrical geometry[7],

$$T(r)=T_W+\frac{\dot{q}'''}{4k}\left(R^2-r^2\right) \qquad (19)$$

RESULTS—Reactor Physics and Design Parameters

A fast spectrum reactor design is desirable, considering the MNR goals of developing a power source that is sustainable, economical, passively safe, secure, and proliferation resistant. Based on Eqns. 15 and 18, we can now quantify the relative impact of various coolants; this is shown in Table II, where, in this example, four fluids (sodium, bismuth, lead-bismuth eutectic (LBE), and lead) are at 600 K and the heating length of the core is 1.0 m.

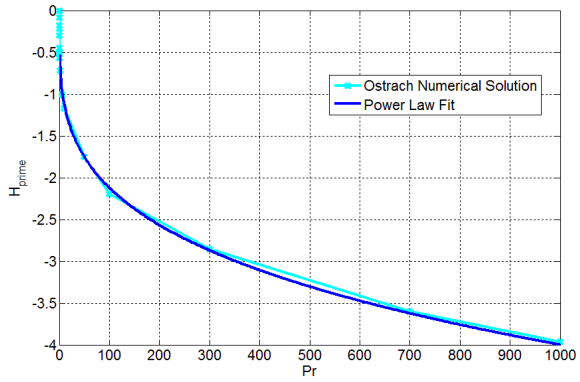

Fig. 4. Dimensionless Temperature vs. Pr.

Table II. Validation of the Fuego Natural Circulation Model (fluid=water).

	Pr	Gr_x	Ra_x	Nu_x	u_{max} (m/s)
Na	0.0054	1.03×10^{12}	5.56×10^{9}	38.0	0.471
Bi	0.018	2.23×10^{12}	3.97×10^{10}	83.4	0.264
LBE	0.021	2.16×10^{12}	4.49×10^{10}	89.4	0.261
Pb	0.026	9.16×10^{11}	2.39×10^{10}	80.6	0.246

As a preliminary analysis design, parameters for a generic fast reactor with a range of thermal output powers were determined by using spectrum-averaged fission cross sections to generate fission reaction rates. An average energy release of 200 MeV per fission was used to attain power level.[9] The results are listed in Table III. As indicated, for a power of 0.5 to 100 MW, the fuel mass would be minimal, ranging from about 100 to 6,000 kg. The lifetime of the core spans from about 3.5 to 10 years with a fast neutron flux having an order of magnitude 10^{14} n/cm^2-s. The MNR shows promise as a reactor that uses small amounts of fuel material, while producing energy for long periods of time without refueling. Additionally, the design can incorporate minimal reactivity swings during the core lifetime, reducing the need for excessive control measures.

Table III. MNR Design Parameters.

Power (MW_{th})	Total Fuel Mass @19.9% U-235 (kg)	Neutron Flux (n/cm^2-s)	Core Life (year)
0.5	105	1.5×10^{14}	10
1.0	135	2.3×10^{14}	7
25	2,000	4×10^{14}	4
100	6,000	5×10^{14}	3.5

Future analysis will include optimization according to desired parameters, which depend on the given MNR application. A range of coolant, fuel, and control options will be included in the assessment. The final design will provide a sustainable energy source that is passively safe, has very low proliferation risk, and is economically advantageous by offering low capital cost and competitive levelized energy costs.

NOMENCLATURE

f' = dimensionless velocity
Gr = Grashof number
H' = dimensionless temperature
h = convective heat transfer coefficient
LBE = lead-bismuth eutectic
LWR = light water reactor
MNR = miniature nuclear reactor
Nu = Nusselt number
Pr = Prandtl number
$\dot{q}'''$ = power per unit volume
R = core radius
Ra = Rayleigh number=GrPr
SMR = small modular reactor

REFERENCES

1. World Nuclear Association, "The Economics of Nuclear Power", http://www.world-nuclear.org/info/Economic-Aspects/Economics-of-Nuclear-Power (2015).

2. Hyperion Power, "Hyperion Launches U2N3-Fueled, Pb-Bi-Cooled Fast Reactor", http://www.neimagazine.com/news/newshyperion-launches-u2n3-fuelled-pb-bi-cooled-fast-reactor (2009).

3. Bloomberg News, "Small Nuclear Reactors Are Becoming Big Business" (2010).

4. Sandia Labs News Release, "Moly 99 Reactor using Sandia Design Could Lead to US Supply of Isotope to Track Disease", https://lockerdome.com/sciencedaily.com/67153467585357 00 (2014).

5. N. OWANO, "Molten Salt Reactor Concept has New Transatomic Power Lift", http://techxplore.com/news/2014-06-molten-salt-reactor-concept-transatomic.html (2014).

6. S. RODRIGUEZ, "Swirling Jets for the Mitigation of Hot Spots and Thermal Stratification in the VHTR Lower Plenum", PhD diss., University of New Mexico (2011).

7. J. HOLMAN, Heat Transfer, 7th Edition, McGraw-Hill, Inc. (1990).

8. S. OSTRACH, "An Analysis of Laminar Free-Convection Flow and Heat Transfer about a Flat Plate Parallel to the Direction of the Generating Body Force", Report 1111, National Advisory Committee for Aeronautics, NASA (1953).

9. J. LAMARSH, A. BARRATTA, Introduction to Nuclear Engineering, 3rd Edition, Prentice Hall, Upper Saddle River, New Jersey (2001).